AECL EACL
AECL Research EACL Recherche

AECL-11034

An Analytic Study of the Injection Steering Magnet for the TASCC Cyclotron

Une étude par analyse de l'aimant de direction du faisceau injecté du cyclotron de TASCC

W.G. Davies

July 1994 juillet

AECL Research

AN ANALYTIC STUDY OF THE INJECTION STEERING MAGNET FOR THE TASCC CYCLOTRON

W.G. Davies

Nuclear Physics Branch
Chalk River Laboratories
Chalk River, Ontario K0J 1J0
1994 July

AECL-11034

EACL Recherche

UNE ÉTUDE PAR ANALYSE DE L'AIMANT DE DIRECTION DU FAISCEAU INJECTÉ DU CYCLOTRON DE TASCC

par

W.G. Davies

RÉSUMÉ

On a effectué une étude par analyse de l'aimant de direction du faisceau injecté N° 2 qui est logé dans la culasse du cyclotron supraconducteur de TASCC. À des champs magnétiques élevés se produisant dans le cyclotron, on a observé que la force de l'aimant de direction était insuffisante pour injecter convenablement le faisceau; on a avancé comme hypothèse que la cause était la saturation de l'aimant du fait de fuites provenant de la culasse du cyclotron. L'étude a confirmé l'hypothèse et, en outre, on a reconçu l'aimant pour éliminer les problèmes mentionnés ci-dessus. On donne des détails sur l'approche par analyse ainsi que les résultats de l'analyse de l'aimant original et de l'aimant reconçu.

Service de Physique nucléaire
Laboratoires de Chalk River
Chalk River (Ontario) K0J 1J0
1994 juillet

AECL-11034

AECL Research

AN ANALYTIC STUDY OF THE INJECTION STEERING MAGNET FOR THE TASCC CYCLOTRON

W.G. Davies

ABSTRACT

A two-dimensional analytic study has been made of the injection steering magnet No. 2, which resides inside the yoke of the TASCC superconducting cyclotron. At high magnetic fields in the cyclotron, it was observed that the steering magnet had insufficient strength to properly inject the beam; saturation of the steering magnet as a result of leakage from the cyclotron yoke was hypothesized as the cause. This hypothesis has been confirmed by this study, and furthermore, the steering magnet has been re-designed to circumvent the above problems. Details of the analytic approach are given along with the results of the analysis of the original and redesigned magnets.

Nuclear Physics Branch
Chalk River Laboratories
Chalk River, Ontario K0J 1J0
1994 July

AECL-11034

CONTENTS

1. INTRODUCTION

It has become apparent during recent attempts to accelerate uranium ions in the TASCC cyclotron [1] that the injection steering magnet (SM-2) does not have sufficient bending power to produce a properly centered beam at injection; this problem is felt to result from saturation of the iron of the steering magnet due to flux leaking from the cyclotron yoke. Furthermore, the aperture of this magnet (1.5 cm) is too small to transmit all of the beam. The steerer sits in a 30 cm diameter hole in the cyclotron yoke (see Figure 1), which at high mean magnetic fields (> 4.5 T) is fully saturated; TOSCA calculations indicate that for a 5 T mean field in the cyclotron, the magnetic field in the yoke is 2.215 T. This saturated condition of the yoke means that a large magnetic field exists in the yoke hole and much of this leakage flux will be carried by the yoke of the steering magnet. Saturation of the yoke of the steering magnet will greatly reduce its bending power when the steering direction is such that the flux from the coils of the steering magnet add to the leakage from the cyclotron.

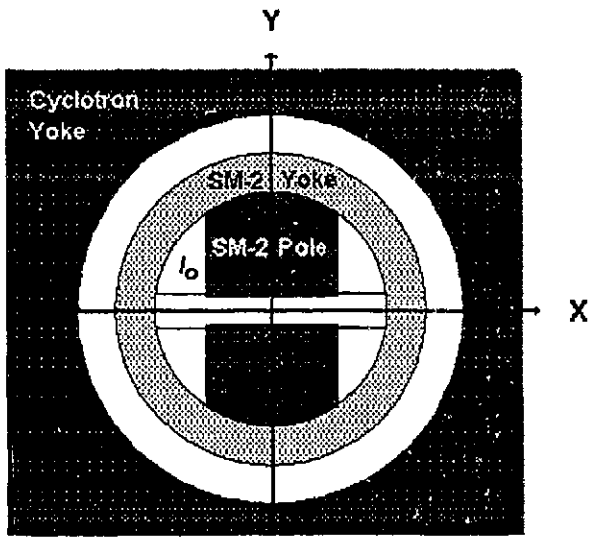

Figure 1 Schematic drawing of the injection steering magnet SM-2.

In order to study this problem and to optimize the design of a replacement magnet, it was felt that an analytic approach would be useful. An analytic solution can be found in two dimensions if we assume uniform permeability; such an assumption, although not completely accurate, will give a good indication of the situation and will allow the yoke of the steering magnet to be optimized.

2. ANALYTIC MODEL

If we assume a uniform magnetic field in the vertical direction in the cyclotron yoke, and neglect for the moment any current in the steering magnet, we can write [2, 3]

$$\mathbf{H} = -\nabla\Phi, \tag{1}$$

where Φ is the magnetic scalar potential which satisfies Laplace's equation

$$\nabla^2\Phi = 0. \tag{2}$$

It is most convenient to use cylindrical coordinates, as this describes the geometry of the yoke-hole and the steering magnet. In cylindrical coordinates (2) becomes

$$\frac{1}{r}\frac{d}{dr}\left[r\frac{d\Phi}{dr}\right] + \frac{1}{r^2}\frac{d^2\Phi}{d\theta^2} + \frac{d^2\Phi}{dz^2} = 0. \tag{3}$$

Separation of variables in the usual way leads to

$$\Phi = R(r)\Theta(\theta)Z(z) \tag{4}$$

which in turn leads to three differential equations

$$\frac{d^2Z}{dz^2} + \nu^2 Z = 0 \tag{5}$$

$$\frac{d^2\Theta}{d\theta^2} + n^2\Theta = 0, \tag{6}$$

and

$$r^2\left[\frac{d^2R}{dr^2}\right] + r\frac{dR}{dr} - \left[\nu^2r^2 + n^2\right]R = 0. \tag{7}$$

In our case, we neglect any z-dependence; in other words, we assume that the hole and the steering magnet are infinitely long. Hence Z = constant, which implies that ν = 0. Thus,

$$Z(z) = e^{i(\nu z + \gamma)} \Rightarrow K = \{constant\} \tag{8}$$

and

$$\Theta(\theta) = e^{in\theta}, \tag{9}$$

For $\nu = 0$, the solution to (7) is

$$R(r) = \mathfrak{C}_n r^n + \mathfrak{D}_n r^{-n} \tag{10}$$

as is easily checked by direct substitution of (10) into (7); $\mathfrak{C}_n$ and $\mathfrak{D}_n$ are real constants.

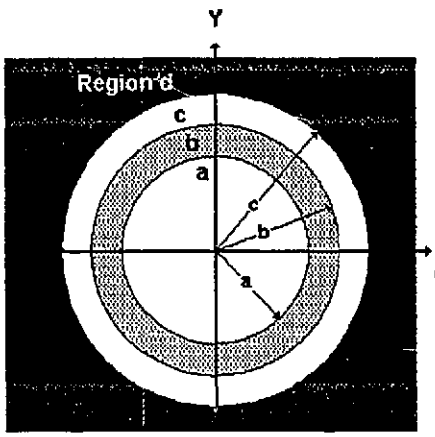

a (mm)	b (mm)	c (mm)
90	120	150

Figure 2 Schematic of a section of the yoke showing the yoke hole, and the steering magnet yoke with poles and coils removed. The radii and regions shown correspond to magnetic field and parameter designations in the text.

If we assume that the field is vertical in the cyclotron yoke for r >> c (see region d of Figure 2) then the potential Φ must have the form

$$\Phi^d = -H_0 r\sin(\theta) + \sum_{n=1}^{\infty} A_n r^{-n} \sin(n\theta) \tag{11}$$

where $\mathcal{E}_1 = H_0$ is the field in the yoke far from the hole and the A_n are constants to be determined; $\mathbf{B}_0 = \mu\mathbf{H}_0$ and the magnetic induction is uniform for r >> c. The general boundary conditions for a static magnetic field are [2]

$$\mathbf{n}\cdot(\mathbf{B}_2 - \mathbf{B}_1) = \mathbf{n}\cdot(\mu_2\mathbf{H}_2 - \mu_1\mathbf{H}_1) = \mathbf{n}\cdot(\mu_2\nabla\Phi_2 - \mu_1\nabla\Phi_1) = 0 \tag{12}$$

and

$$\mathbf{n}\times(\mathbf{H}_2 - \mathbf{H}_1) = \mathbf{n}\times(\nabla\Phi_2 - \nabla\Phi_1) = \mathbf{K}, \tag{13}$$

where **n** is a unit vector perpendicular to the boundary and **K** is the surface current on the boundary. For b < r < c, both of the solutions to the Bessel equation (7) are allowed, and from the boundary conditions we see that the potential has the form

$$\Phi^c = \sum_{n=1}^{\infty} \left[B_n r^m + C_n r^{-n}\right] \sin(n\theta). \tag{14}$$

Similarly, in region b, a < r < b the potential has the form

$$\Phi^b = \sum_{n=1}^{\infty} \left[D_n r^n + E_n r^{-n} \right] \sin(n\theta) \tag{15}$$

and in region a, $0 < r < a$, Φ has the form

$$\Phi^a = \sum_{n=1}^{\infty} F_n r^n \sin(n\theta) \tag{16}$$

because Φ must be finite at the origin. In order to determine the unknown coefficients A_n through F_n, we must set up a system of equations that satisfy all of the boundary conditions simultaneously. From the symmetry of the problem, we see that the normal boundary condition (12) is satisfied by B_r and the tangential boundary condition (13) is satisfied by H_θ, where the subscripts r and θ refer to the radial and tangential components of **B** and/or **H** in cylindrical coordinates. The gradient in cylindrical coordinates is [4]

$$\nabla\Phi = \hat{r}\frac{\partial\Phi}{\partial r} + \hat{\theta}\frac{1}{r}\frac{\partial\Phi}{\partial\theta} \tag{17}$$

which leads to the following components for H:

$$H_r^d = -\frac{\partial\Phi^d}{\partial r} = H_0\sin(\theta) + \sum_{n=1}^{\infty} nA_n r^{n-1} \sin(n\theta) \tag{18}$$

$$H_\theta^d = -\frac{1}{r}\frac{\partial\Phi^d}{\partial\theta} = H_0\cos(\theta) - \sum_{n=1}^{\infty} nA_n r^{n-1} \cos(n\theta) \tag{19}$$

$$H_r^c = -\sum_{n=1}^{\infty} n\left[B_n r^{n-1} - C_n r^{-n-1} \right] \sin(n\theta) \tag{20}$$

$$H_\theta^c = -\sum_{n=1}^{\infty} n\left[B_n r^{n-1} + C_n r^{-n-1} \right] \cos(n\theta) \tag{21}$$

$$H_r^b = -\sum_{n=1}^{\infty} n\left[D_n r^{n-1} - E_n r^{-n-1} \right] \sin(n\theta) \tag{22}$$

$$H_\theta^b = -\sum_{n=1}^{\infty} n\left[D_n r^{n-1} + E_n r^{-n-1}\right]\cos(n\theta) \tag{23}$$

$$H_r^a = -\sum_{n=1}^{\infty} nF_n r^{n-1}\sin(n\theta) \tag{24}$$

$$H_\theta^a = -\sum_{n=1}^{\infty} nF_n r^{n-1}\cos(n\theta) \tag{25}$$

3. FIELDS IN THE CYCLOTRON YOKE HOLE

It is instructive to study first the simple problem of just the hole in the yoke with no surface currents present; here we need only the solutions for regions d and a. From the boundary conditions, we obtain the equations

$$k_d\left[H_0\sin(\theta) + \sum_{n=1}^{\infty} nA_n r^{n-1}\sin(n\theta)\right] = -\sum_{n=1}^{\infty} nF_n r^{n-1}\sin(n\theta) \tag{26}$$

and

$$H_0\cos(\theta) - \sum_{n=1}^{\infty} nA_n r^{-n-1}\cos(n\theta) = -\sum_{n=1}^{\infty} nF_n r^{n-1}\cos(n\theta) \tag{27}$$

where we assume no currents on the boundary; $k_d = \mu_d/\mu_0$, the ratio of the permeability of region d to the permeability of free space. Equations (26) and (27) can be rewritten as an infinite set of matrix equations of the form $\mathcal{H}^n = \mathcal{M}^n C^n$ as follows:

$$\begin{bmatrix} k_d H_0 \\ H_0 \end{bmatrix} = \begin{bmatrix} -k_d/c^2 & -1 \\ 1/c^2 & -1 \end{bmatrix}\begin{bmatrix} A_1 \\ F_1 \end{bmatrix} \tag{28}$$

$$\begin{bmatrix} 0 \\ 0 \end{bmatrix} = \begin{bmatrix} -k_d/c^{n+1} & -1/c^{n-1} \\ 1/c^{n+1} & -1/c^{n-1} \end{bmatrix}\begin{bmatrix} A_n \\ F_n \end{bmatrix};\ n > 1. \tag{29}$$

where we equate the coefficients of $\sin(n\theta)$ and $\cos(n\theta)$, respectively, for each value

of n. We see from (29) that F_n and A_n vanish for all n > 1. The inverse of the matrix in (28) is easily found to be

$$\mathcal{M}^{-1} = \frac{1}{k_d+1}\begin{bmatrix} -c^2 & c^2 \\ -1 & -k_d \end{bmatrix} \tag{30}$$

where we have dropped the superscript on the vectors and matrices. Hence the coefficients are $C = \mathcal{M}^{-1}\mathcal{H}$ with $\mathcal{H}^T = (k_d H_0, H_0)$ and we obtain

$$A_1 = \frac{c^2 H_0(1-k_d)}{k_d+1}, \quad F_1 = -\frac{2k_d H_0}{k_d+1}. \tag{31}$$

We see that in the limit $k_d \rightarrow 1$ that $A_1 \rightarrow 0$ and $F_1 \rightarrow -H_0$, as expected.

Also from (24) and (25) we see that the magnetic field **H** and the induction **B** are uniform everywhere in the hole in the yoke (region a) as long as the permeability is constant, which is a good approximation either when the yoke is fully saturated or when the yoke is well below saturation and the relative permeability is very high, >1000. As we approach saturation, the permeability will be a complicated function of r and θ and will result in terms with n > 1 being non-zero.

3.1 Simple cos(θ) Current Distribution

If we add a surface-current density in the z-direction of the form $I_0/c\ \cos(\theta)$ on the boundary r = c, we find from (13) and (27) that the matrix $\mathcal{M}$ remains unchanged, but the "driving-vector" $\mathcal{H}$ becomes $\mathcal{H}^T = (k_d H_0, H_0 + I_0/c)$. We obtain immediately the new coefficients

$$A_1 = \frac{c[cH_0(1-k_d)+I_0]}{k_d+1}, \quad F_1 = -\frac{k_d(2cH_0+I_0)}{c(k_d+1)}. \tag{32}$$

This result shows directly that a cos(θ) current distribution produces a perfect dipole field in a linear system. Depending on the sign, the current I_0 adds to or subtracts from the imposed field, as expected.

4. ANALYSIS OF THE STEERING MAGNET SM-2

4.1 Analysis of the Original Design

We now turn to the original problem of the steering magnet in the hole. For the purposes of this analysis, we will ignore the poles in the original steering magnet (see Figure 1) and treat only the yoke; if the yoke is saturated, then the magnet will not generate the required steering fields. The important parameters of the present steering magnet are shown in Table 1, while Figure 2 shows the geometry under investigation as well as the definitions of important regions and parameters.

Table 1
Parameters for the Present Magnet

FIELD	2 COILS		POLE			YOKE	
B (T)	A-t (A)	Gap (mm)	Width (mm)	Length (mm)	Inner ϕ(mm)	Outer ϕ(mm)	Hole ϕ(mm)
1.00	22060	20.0	50.0	140.0	18.00	24.00	30.00

By arguments identical to the ones above, we conclude that all coefficients are zero for n > 1. Hence from (18) through (25) and the boundary conditions, we obtain the following matrix $\mathcal{M}$ for the coefficients $A_1 \rightarrow F_1$:

$$\mathcal{M} = \begin{bmatrix} -k_d/c^2 & -1 & 1/c^2 & 0 & 0 & 0 \\ 1/c^2 & -1 & -1/c^2 & 0 & 0 & 0 \\ 0 & -1 & 1/b^2 & k_b & -k_b/b^2 & 0 \\ 0 & -1 & -1/b^2 & 1 & 1/b^2 & 0 \\ 0 & 0 & 0 & k_b & -k_b/a^2 & -1 \\ 0 & 0 & 0 & 1 & 1/a^2 & -1 \end{bmatrix} \tag{33}$$

Here, $k_d = \mu_d/\mu_0$, and $k_b = \mu_b/\mu_0$, the ratios of the permeabilities of regions d and b, respectively, to the permeability of free space. If we add, as in the above discussion, a current-density of the form $I_0/a \cos(\theta)$ flowing in the z-direction on the boundary r = a, we see that $\mathcal{H}^T = (k_d H_0, H_0, 0, 0, 0, I_0/a)$. The matrix, $\mathcal{M}$, can be inverted with the help of the MAPLE-V algebra program. The result is very complicated and it is not meaningful to display it. The expressions for the coefficients $A_1 \rightarrow F_1$ are given in Appendix 1. The advantage of the analytic approach is that we can easily compute the fields as a function of a, b, H_0 and I_0 in any desired combination.

Our first task is to estimate the main parameters of the model. The yoke fields B_{yoke} were calculated with the program TOSCA [4], which incorporated a standard B-H curve with a saturation magnetization $\mu_0 M_s = 2.14$ T. From the relation between **B** and **H** and the definition of magnetization, we see that far from the hole,

$$H_0 = B_{yoke}/\mu_d \tag{34}$$

These quantities can be obtained from a B-H curve. The B-H curve for the iron used in the cyclotron was never measured. What is known is that the saturation magnetization of a sample of the yoke iron was $\mu_0 M = 2.12$ T, instead of the more typical 2.14 T for pure iron. Figure 3 shows the "standard" B-H curve and the magnetization curve M from the program POISSON. The curves shown in Figure 3 are used in this analysis. A similar curve is used in TOSCA. In order to compute the solution

$$C = \mathcal{M}^{-1}\mathcal{H} \tag{35}$$

to the matrix equation $\mathcal{H} = \mathcal{M}C$, we must determine the relative permeabilities, k_d and k_b. For the purposes of this discussion, we assume the value that k_d has far from the

hole; this will underestimate the flux leaking into the hole. The constant k_b must be found by an iterative procedure; we assume a magnetization M and then solve the equations

$$\mu_0 \mathbf{M} = \mathbf{B} - \mu_0 \mathbf{H}; \quad \mathbf{B} = \mu \mathbf{H} \tag{36}$$

which leads to

$$\mathbf{M} = (k_b - 1)\mathbf{H} \tag{37}$$

where **H** is also a function of k_b. Because **M** is very near the saturation magnetization $\mathbf{M}_s$, the system converges very rapidly (see Figure 3). The value of k_b is computed at the mean radius of the steering magnet yoke; (a+b)/2.

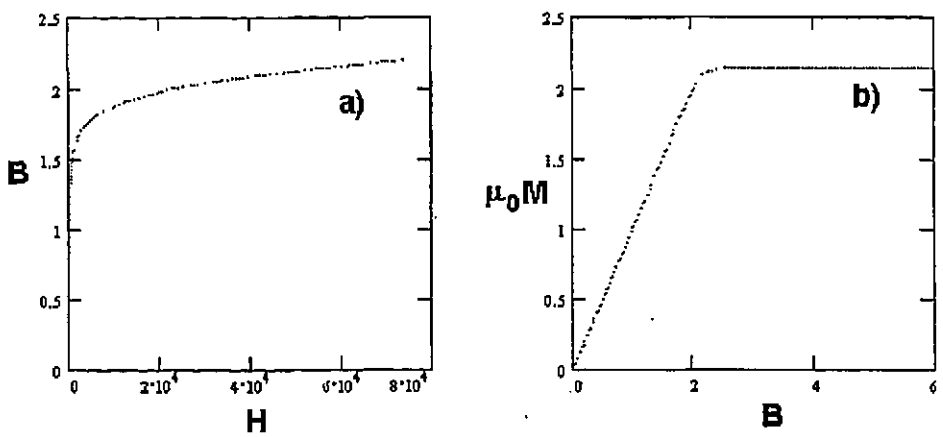

Figure 3 a) A typical B-H curve for pure iron, taken from the program POISSON. b) The Magnetization curve derived from the B-H curve shown in frame a).

Table 2 gives the important parameters used in the calculations along with the principal results of the model shown in Figure 2. Figure 4 plots **B**, for $\mathbf{B}_{mean}$ = 5 T, as a function of r on the horizontal plane, where the fields are a maximum, for the four regions shown in Figure 2. We see immediately from Figure 4 and Table 2 that in the vicinity of the midplane, the yoke of the steering magnet is saturated for the high field case at all radii even without any steering current. Figure 5a shows a 3-D plot of the magnetic intensity $|\mathbf{B}|$ as a function of r and θ for the yoke of the steering magnet at the high-field; Figure 5b shows $|\mathbf{B}|$ as a function of r for $\theta = \pi/2$, *i.e.* along the valley of Figure 5a where the boundary condition on the normal component of **B**, (12), applies. This result confirms that the bending power of the steering magnet will be greatly reduced for high mean fields in the cyclotron due to saturation of its yoke. Figure 6 shows a similar plot to Figure 4 for $\mathbf{B}_{mean}$ = 3.6 T. Here we see that the leakage flux into the hole is small and that the steering magnet yoke fields are modest; there is no difficulty reaching the full steering power in this case.

Table 2
Principal Parameters for Original Magnet

B_{mean}(1) (T)	B_{yoke}(2) (T)	H_0 (A/m)	B_a (T)	B_b (T)	k_b	k_d
5	2.215	81715.6	0.1035	2.196	24.311	21.616
3.6	1.603	1662.15	1.55×10^{-4}	0.09119	6787.0	767.92

(1) Mean Magnetic Induction B in the accelerating region of the cyclotron.
(2) Magnetic Induction B in the Cyclotron yoke far from the hole.

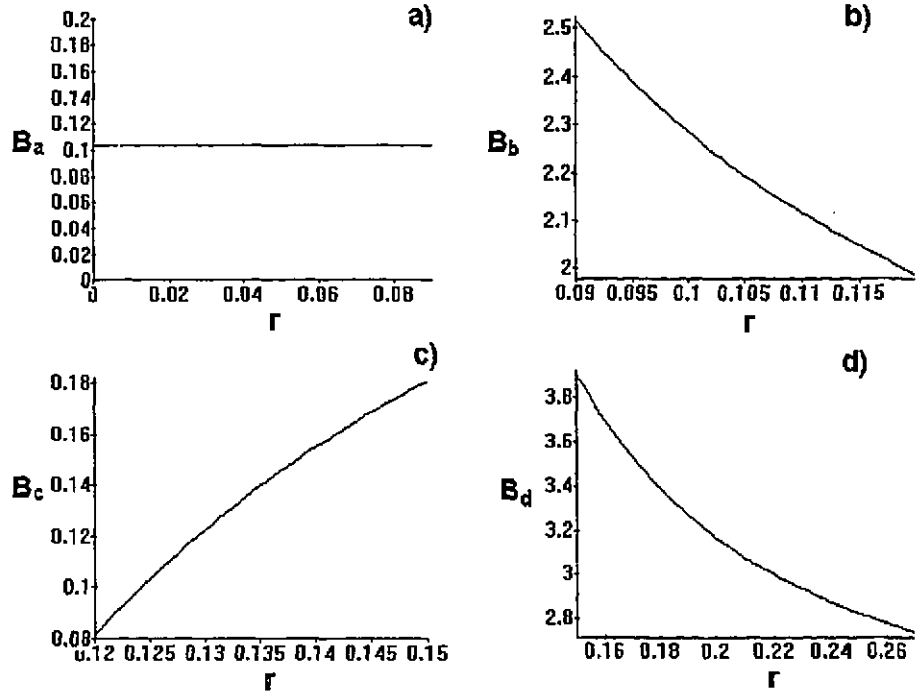

Figure 4 Magnetic induction **B**(T) for the original design at B_{mean} = 5 T as a function of r for θ = 0; a) region a, b) region b, c) region c, and d) region d. Note that the yoke of the steering magnet, b), is saturated.

4.2 Design Optimization

The first question one can ask is "Is it possible to modify the yoke design of the present magnet to reduce the saturation?". Figure 7 shows k_b, B_b, and B_a as a function of the outer radius of the steering magnet yoke. The figure shows that for a fixed value of a = 0.09 m, which is determined by the pole and coil requirements, the value b = 0.12 m is optimum. Either an increase or a decrease in b leads to a reduction in k_b and a corresponding increase in B_b, and B_a. Thus it is not possible to improve the current design.

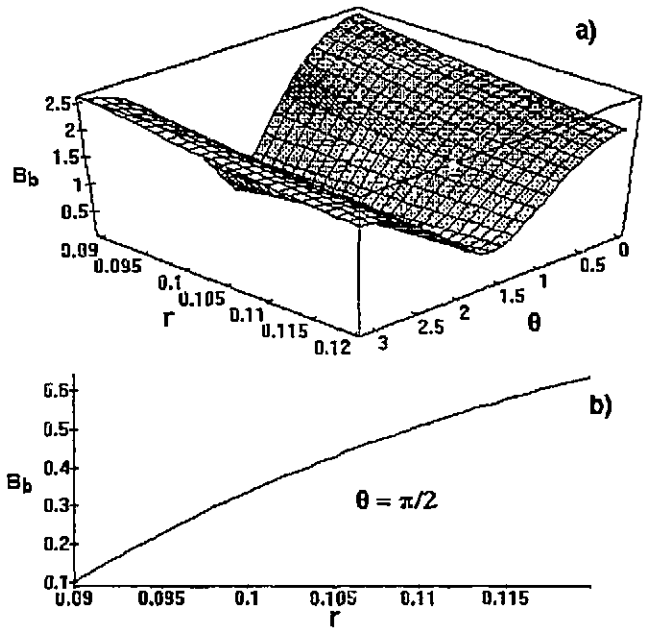

Figure 5 Fields in region b: a) Isometric plot of $|\mathbf{B}|$ as a function of θ. b) Plot of $|\mathbf{B}|$ as a function of r, a < r < b, which lies along the valley of a).

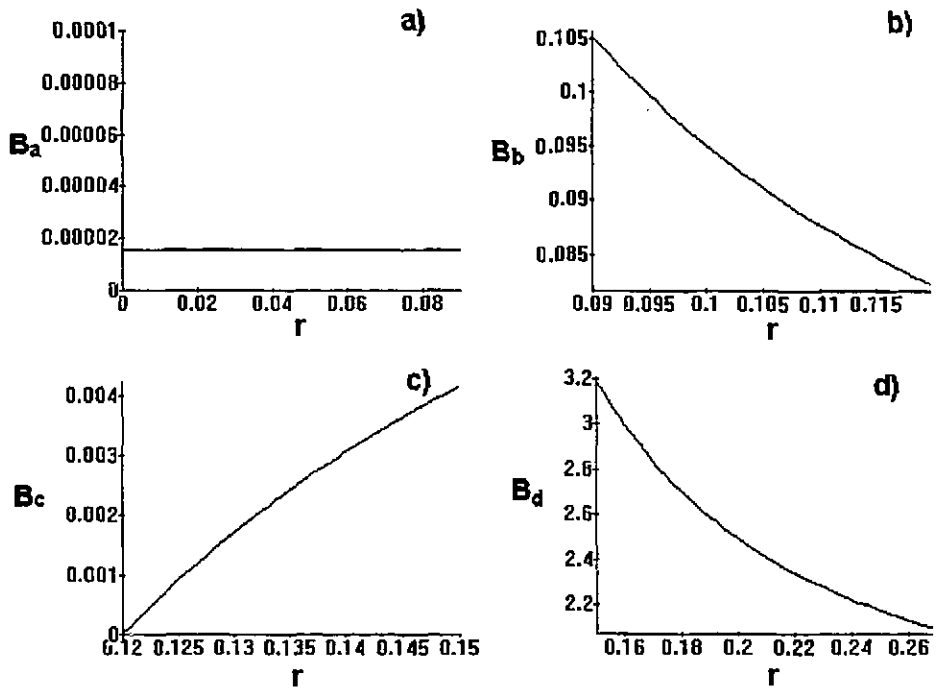

Figure 6 Magnetic induction **B** for the original design at $\mathbf{B}_{mean}$ = 3.6 T as a function of r for θ = 0; a) region a, b) region b, c) region c, and d) region d.

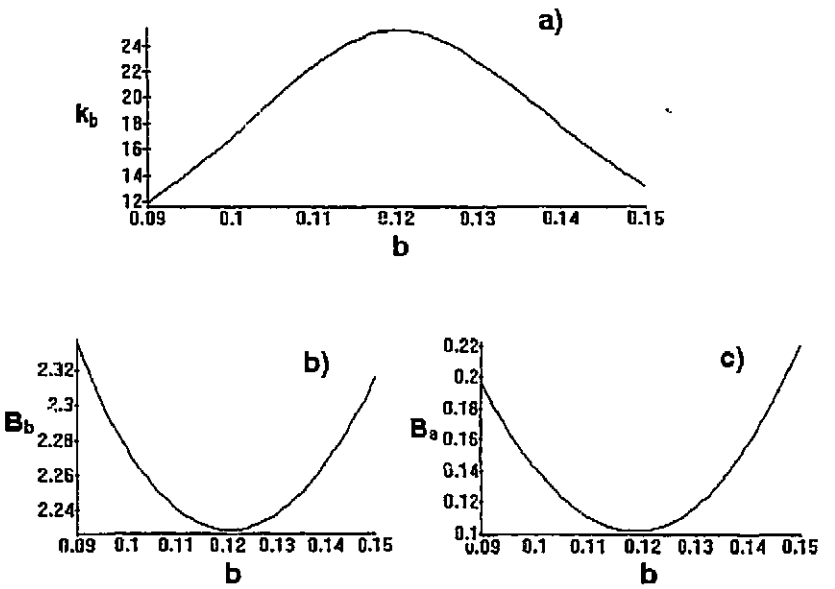

Figure 7 Optimization of radius b for the original design at B_{mean} = 5 T: a) The relative permeability k_b as a function of the outer yoke radius; a < b < c. b) The magnetic induction B_b in the midplane of the steering magnet yoke. c) B_a in the interior of the steering magnet.

The only way to improve the performance is to decrease the inner radius, a, which leaves too little room for the coils in a conventional magnet. Also, the aperture should be increased as much as possible to improve the beam transmission. Since the injection steering magnet is preceded by a vertical steering magnet, another improvement would be to combine the X- and Y-plane steerers into one unit. This would allow us to lengthen the combined magnet, which would result in greater shielding of the leakage flux and decrease the maximum fields required in both the X and Y directions. The solution to this problem is to employ a double "Cos(θ)" type of magnet, which, as we will see, requires superconducting coils.

Let us combine the vertical and horizontal magnets and increase the length from 140 mm to 350 mm. Because the bending power of the magnet varies as BL/Bρ, where L is the length of the magnet and Bρ is the magnetic rigidity of the beam, we could reduce the field by 140/350; let us choose 1/2, as it gives us an extra margin. If we assume that a clear aperture of 40 mm is adequate (the present magnet has a useful aperture of less than 15 mm), and that the coils and their constraints can be wound into a 25 mm space, then the yoke of the steering magnet can be thickened and its outer radius re-optimized. Here, though, we will include the field from the coils of the steering magnet; this strategy minimizes the field in the steering magnet yoke and hence the perturbation of the field in the cyclotron yoke due to the steering magnet. Perturbation of the cyclotron yoke field induces a first harmonic in the cyclotron midplane field and will decenter the beam. Let us assume that the new inner radius of

the steering magnet yoke is a = 50 mm; then, following the procedures used to obtain Figure 7, we find from Figure 8 that the optimum is around b = 105 mm, which includes now the effect of the maximum steering field of 0.5 T.

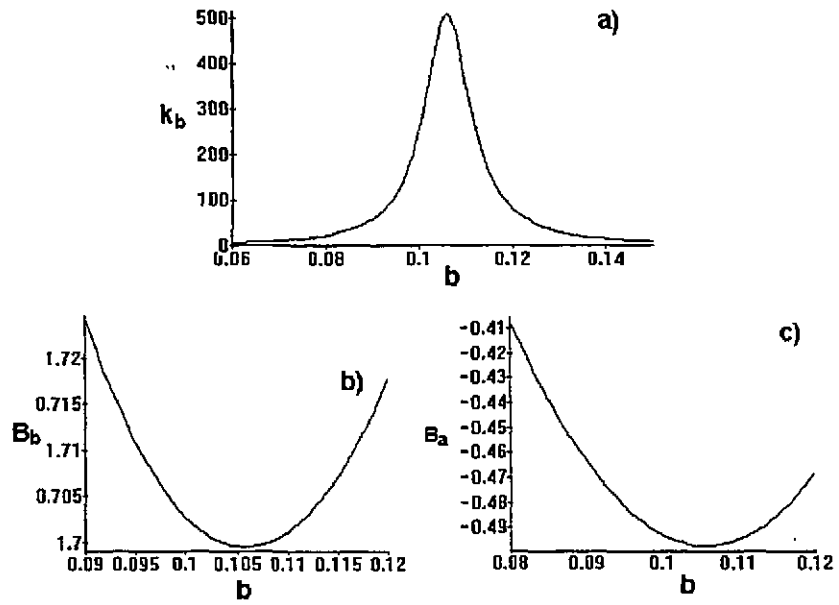

Figure 8 Optimization of radius b for the improved design at $\mathbf{B}_{mean}$ = 5 T: a) The relative permeability k_b as a function of the outer yoke radius; a < b < c. b) The magnetic induction $\mathbf{B}_b$ in the midplane of the steering magnet yoke. c) B_a in the interior of the steering magnet.

Figure 9 shows the geometry of the improved design, while Figure 10 shows the mid-plane fields for the improved design. A comparison of Figure 4 with Figure 10 shows how dramatic the improvements are. The leakage field in the center of the magnet drops to 0.842 mT from 104 mT, while the field in the center of the steerer yoke drops to 1.296 T from 2.196 T. This improvement is mainly the result of the increase in the gap between the steering magnet and the yoke of the cyclotron, which reduces the leakage of flux into the steering magnet, but the increase in thickness of the steering magnet yoke also contributes. Figures 11 and 12 show the operation of the COS(θ) magnet for $\mathbf{B}_{mean}$ = 5 T and I_0 = -20 000 A and I_0 = +20 000 A, respectively. We see that the fields in the active volume of the magnet (region a) lie slightly below and above 0.5 T, respectively. However, the steerer yoke fields are dramatically different, with the yoke partially saturated for I_0 = -20 000 A and below 1 T for I_0 = +20 000 A (see Figure 11 and Figure 12). The perturbation to the field in the cyclotron yoke is now insignificant even for the case with I_0 = -20 000 A shown in Figure 11, although there is some asymmetry between I_0 = -20 000 A and I_0 = +20 000 A. Figures 13 and 14 show the operation of the COS(θ) magnet for $\mathbf{B}_{mean}$ = 3.6 T and I_0 = -20 000 A and I_0 = +20 000 A, respectively. Here we see that the steering magnet operates in a nearly symmetric manner, far from saturation and with no perturbation of the field in the cyclotron yoke. The results for the re-designed steering magnet are given in Table 3.

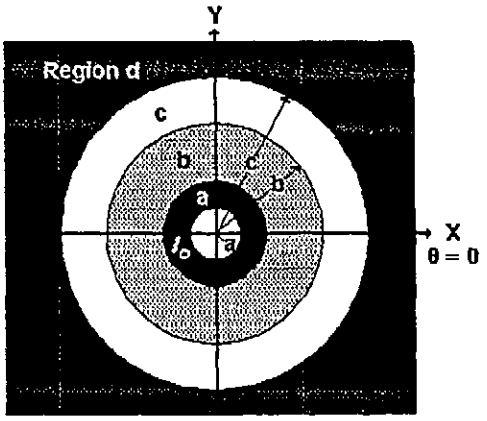

a (mm)	b (mm)	c (mm)
50	105	150

Figure 9 Schematic of a section of improved steering magnet showing the cyclotron yoke, the yoke hole, the steering magnet yoke and superconducting coils. The radii and regions shown correspond to magnetic field and parameter designations in the text.

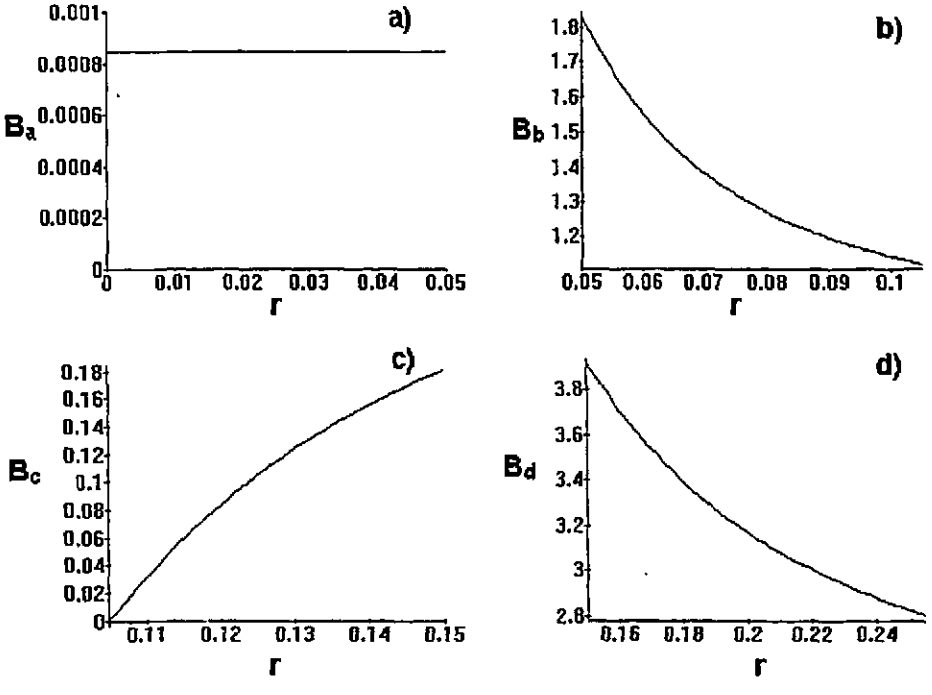

Figure 10 Magnetic induction **B**(T) for the improved design at B_{mean} = 5 T as a function of r for θ = 0; a) region a, b) region b, c) region c, and d) region d.

Table 3
Principal Results for the Improved Magnet

B_{mean}(1) (T)	B_{yoke}(2) (T)	I_0 (A)	B_a (T)	B_b (T)	k_b	k_d
5	2.215	0	0.000842	1.296	24.311	21.616
5	2.215	-20000	-0.4969	1.698	453.0	21.616
5	2.215	+20000	0.5030	0.8800	3447	21.616
3.6	1.603	0	6.2×10^{-6}	0.02987	6787.0	767.92
3.6	1.603	-20000	-.5025	0.4473	4336	767.92
3.6	1.603	+20000	+.5025	0.4473	4336	767.92

(1) Mean Magnetic Induction B in the accelerating region of the cyclotron.
(2) Magnetic Induction B in the Cyclotron yoke far from the hole.

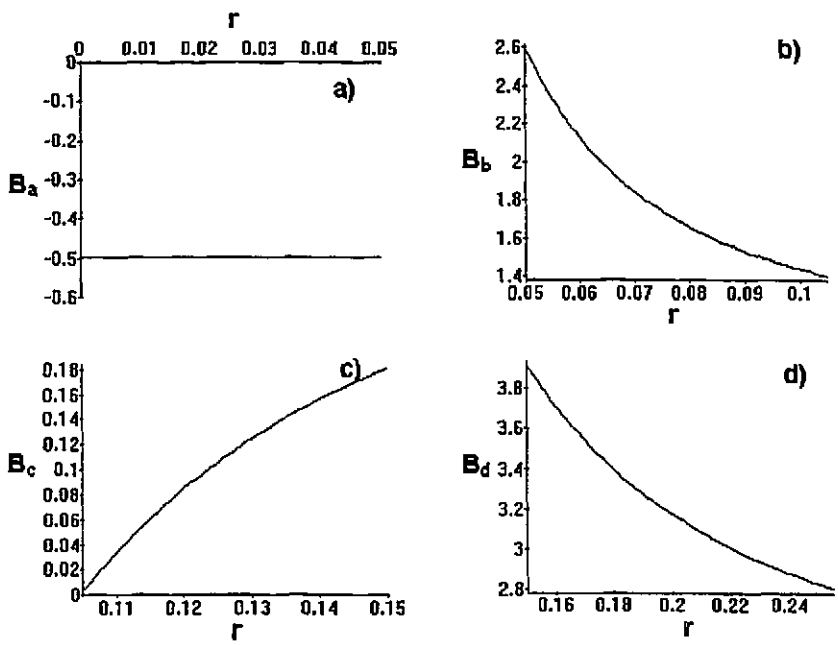

Figure 11 Magnetic induction **B** (T) for COS(θ) steerer at $\mathbf{B}_{mean}$ = 5 T incorporating the improved design as a function of r for θ = 0; a) region a, b) region b, c) region c, and d) region d. The current density has the form $I_0\cos(\theta)/a$ with I_0 = -20 000 A.

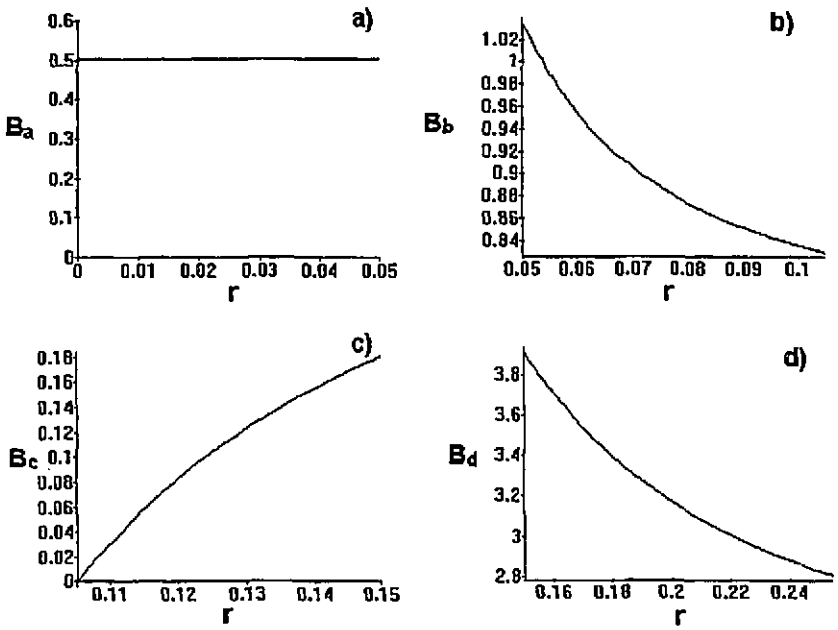

Figure 12 Same as Figure 10, but with I_0 = +20 000 A.

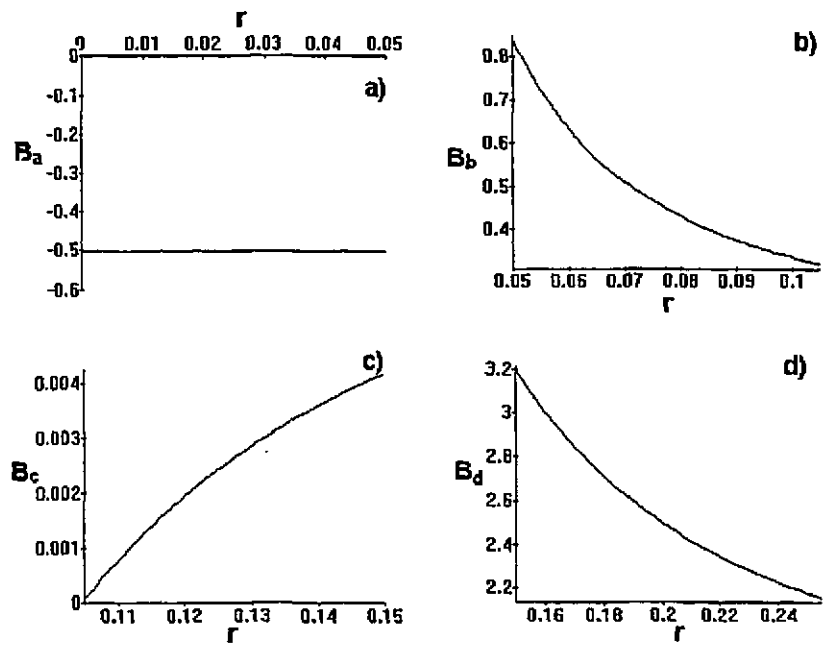

Figure 13 Magnetic induction **B** (T) for COS(θ) steerer at $\mathbf{B}_{mean}$ = 3.6 T incorporating the improved design as a function of r for θ = 0; a) region a, b) region b, c) region c, and d) region d. The current density has the form $I_0\cos(\theta)/a$ with I_0 = -20 000 A.

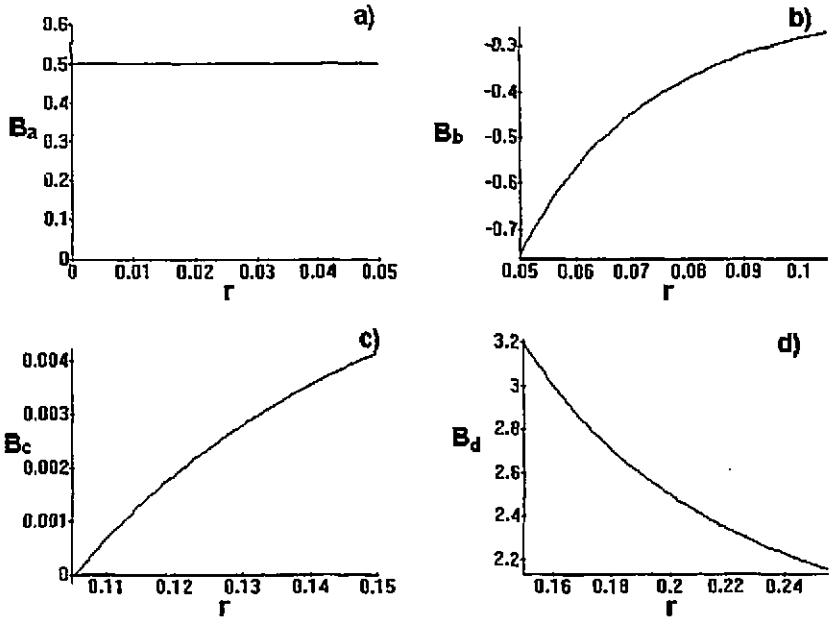

Figure 14 Same as Figure 10, but with I_0 = +20 000 A.

5. CONCLUSIONS

The results presented here show that it is possible to redesign the injection steering magnet SM-2 to reach its design field of ±0.5 T even at maximum cyclotron field. This can be done by making use of a COS(θ)-type magnet. With a maximum current I_0 = 20 000 A, the mean current density is

$$J_0 = I_0 \Big/ \left\{ \int_0^{\pi/2} \int_{r_1}^{r_2} \cos(\theta) r \, d\theta \, dr \right\} = \frac{2I_0}{(r_2^2 - r_1^2)} \tag{38}$$

where r_2 and r_1 are the outer and inner radii of the coil region, respectively. For a conventional coil, we obtain a mean current density of about 20 A/mm². When we account for insulation, and the water channel area, we would obtain a current density of about 50 A/mm², a value well above the current carrying capacity of copper (10-12 A/mm²). Thus, even though we have more than doubled the length of the magnet, and thereby halved the maximum field, the current density is well outside the range for a conventional magnet. (For comparison, the present magnet has 1103 turns per coil of #16 B&S gauge wire, which at a maximum current of 10 amps has a current density of 7.64 A/mm².) This confirms the necessity of using superconducting coils. In order to make superconducting coils stable in this geometry, the coils must be held in a rigid stainless-steel collar. Let us assume that the collar restricts the superconducting windings to a space between r = 30 mm and 40 mm. Then we obtain a mean current density of 57 A/mm². If we assume a packing fraction of 75% for the windings in the coils, we obtain 76 A/mm², far below the current limit of about 2500 A/mm² for NbTi

superconductors. Thus it should be easy to design coils for a combined X-Y COS(θ)-type superconducting steerer. A reasonable design could have 200 turns per coil at 100 A to achieve the required 20 000 A-turns per coil. The vertical steerer coils could be smaller, say 15 000 A-turns per coil as the steering requirements are lower. The above estimate of the required Ampere-turns is only approximate; the value comes from a surface current at r = 50 mm. The real coils will be at a smaller radius, which would reduce the required ampere-turns, but would be decoupled from the iron yoke by the retaining collar, which tends to increase the required ampere-turns.

Although this work demonstrates the possibility of building such a magnet, much more needs to be done. Proper calculations with POISSON, for example, are required for the detailed coil design, not only to determine the conductor geometry and determine the exact value of the A-turns, but to take account of the non-linearities in the iron. A detailed coil design is necessary, which must include a comprehensive stress analysis. The coils must be rigidly clamped so that no conductor motion is possible when the magnet is energized; the energy of a dropped paper clip can quench a superconducting magnet. Also, the cryogenic problems are not insignificant, although certainly solvable.

6. REFERENCES

[1] H. Schmeing, et al., Current Status of the Superconducting Cyclotron at Chalk River, Twelfth Int. Conf. on Cycl. and their Appl., Berlin, 1989.

[2] J.D. Jackson, Classical Electrodynamics, Wiley, 1962. W.K.H. Panofsky and M. Phillips, Classical Electricity and Magnetism, Addison-Wesley, 1961.

[3] The Theory of the Measurement of Magnetic Multipole Fields with Rotating Coil Magnetometers, W.G. Davies, Nucl. Instr. & Meth. A311(1992)399.

[4] N.J. Diserens, private communication; TOSCA is a product of Vector Fields, Kidlington, Oxford, U.K.

APPENDIX 1

Following are the expressions for the coefficients A_1 through F_1 taken from a MAPLE V program used to invert the matrix (33).

$$A_1 = -\frac{c^2 H_0}{Den}\left(2\,k_4\,c^2b^2k_2 + k_4\,c^2b^2 + 2\,k_4\,c^2k_2\,a^2 - k_4\,c^2a^2 + k_4\,c^2b^2{k_2}^2 + k_4\,b^4 - k_4\,a^2b^2 - k_4\,b^4{k_2}^2 + k_4\,b^2{k_2}^2a^2 - 2\,c^2b^2k_2 - c^2b^2 - 2\,c^2k_2\,a^2 + c^2a^2 - c^2b^2{k_2}^2 + c^2{k_2}^2a^2 + b^4 - a^2b^2 - b^4{k_2}^2 + b^2{k_2}^2a^2\right)$$

$$B_1 = \frac{2\,c^2\left(-2\,b^2k_2 - b^2 - 2\,k_2\,a^2 + a^2 - b^2{k_2}^2 + {k_2}^2a^2\right)k_4\,H_0}{Den}$$

$$C_1 = -\frac{2\,c^2\left(b^2 - a^2 - b^2{k_2}^2 + {k_2}^2a^2\right)b^2k_4\,H_0}{Den}$$

$$D_1 = -\frac{4\,c^2b^2\left(k_2+1\right)k_4\,H_0}{Den}$$

$$E_1 = -\frac{4\,c^2b^2\left(k_2-1\right)a^2k_4\,H_0}{Den}$$

$$F_1 = -\frac{8\,k_4\,c^2b^2k_2\,H_0}{Den}$$

$$Den = 2\,k_4\,c^2b^2k_2 + k_4\,c^2b^2 + 2\,k_4\,c^2k_2\,a^2 - k_4\,c^2a^2 + k_4\,c^2b^2{k_2}^2 - k_4\,c^2{k_2}^2a^2 + k_4\,b^4 - k_4\,a^2b^2 - k_4\,b^4{k_2}^2 + k_4\,b^2{k_2}^2a^2 + 2\,c^2b^2k_2 + c^2b^2 + 2\,c^2k_2\,a^2 - c^2a^2 + c^2b^2{k_2}^2 - c^2{k_2}^2a^2 - b^4 + a^2b^2 + b^4{k_2}^2 - b^2{k_2}^2a^2$$

Cat. No. /No de cat.: CC2-11034E
ISBN 0-660-15750-0
ISSN 0067-0367

To identify individual documents in the series, we have assigned an AECL- number to each.

Please refer to the AECL- number when requesting additional copies of this document from:

Scientific Document Distribution Office (SDDO)
AECL Research
Chalk River, Ontario
Canada K0J 1J0

Fax: (613) 584-1745 Tel.: (613) 584-3311 ext. 4623

Price: A

Pour identifier les rapports individuels faisant partie de cette serie, nous avons affecté un numéro AECL- à chacun d'eux.

Veuillez indiquer le numéro AECL- lorsque vous demandez d'autres exemplaires de ce rapport au:

Service de Distribution des Documents Officiels
EACL Recherche
Chalk River (Ontario)
Canada K0J 1J0

Fax: (613) 584-1745 Tél.: (613) 584-3311 poste 4623

Prix: A